Constrained attitude control of agile spacecraft using CMGs

Qiang Shen
Temasek Laboratories
National University of Singapore
Singapore, Singapore 117411
Email: tslshen@nus.edu.sg

Cher Hiang Goh, Chengfei Yue
Department of Electrical and Computer Engineer
National University of Singapore
Singapore, Singapore 117582
Email: elegch@nus.edu.sg; e0011355@u.nus.edu

***Abstract*—This paper investigates rest-to-rest attitude reorientation problem for an agile spacecraft in the presence of attitude-constrained zones. Since agile spacecraft require an attitude control system that provides rapid rotational maneuverability and tracking capability, control moment gyro (CMG) is often considered as ideal torque-generating actuators. Specifically, based on a quadratic potential function, a nonlinear attitude controller is developed to avoid the undesired celestial objects autonomously while achieving asymptotic attitude stabilization. Then, general singular robust (GSR) steering logic is employed to determine the CMG gimbal rate commands that can generate the commanded spacecraft control torques from attitude controller. The proposed attitude control scheme has simple structure, which is of great interest for aerospace industry when onboard computing power is limited. Finally, simulation results for a CMG-based spacecraft are presented to show the effectiveness of the proposed attitude control systems.**

I. Introduction

Future spacecraft require to have a smaller size while achieving rapid rotational agility and high pointing accuracy [1]. Control moment gyros (CMGs) are known to provide higher slew rate and torque output for the same amount of power comparing to reaction wheels, which makes it highly desirable for space missions with rapid slew rates and high pointing accuracy requirements. In the past two decades, CMGs have been successfully employed for a variety of large spacecraft, such as the Skylab, the MIR space station, and the International Space Station. For small satellite, using CMGs as actuators is still in the process of laboratory test.

One of the difficulties associated with CMGs is the occurrence of singularity states, at which CMGs are unable to exactly produce the required torque in certain directions. In order to overcome CMGs singularity problem, several papers present various solutions such as singular escape method [2], [3] and singular avoidance method [4]–[6]. Singular avoidance method uses offline calculation to search gimbal path trajectories so that the CMG systems do not encounter any singularity globally. However, this method is fairly complex and not suitable for real-time computation. On the other hand, singular avoidance method has a simple structure and doesn't need offline calculation. Although singular avoidance method may introduce certain torque errors in the presence of singularity, the overall control performance could be satisfactory [7].

In practical spacecraft systems, one of their essential functions is to point an on-board instrument's boresight along a prescribed inertial direction [8]. In such a mission, instruments equipped on the spacecraft are sensitive payloads that are required to be kept sufficiently far away from unwanted celestial objects or bright source of energy. In view of this requirement, the capacity of attitude controller to handle attitude constraints should be guaranteed. Otherwise, it will lead to damage of certain payloads and inferior control performance. For example, the infrared telescopes may be required to slew from one direction in space to another without direct exposure to the sun vector or other infrared bright regions [9]–[11]. Generally, this type of attitude maneuver can be regarded as a spacecraft reorientation problem in the presence of attitude-constrained zones and has attracted more and more attention in practical spacecraft missions. Potential function method formulates the attitude constrained zones in the context of an artificial potential, which is further used for synthesizing the corresponding attitude control law to avoid unwanted celestial objects. It is analytical without the need of any change in the overall structure of the attitude control software or hardware,which makes it suitable for on-board computation and provides flexible autonomous operations [12].

This paper presents a potential function based attitude controller to achieve rest-to-rest attitude slew and avoid the attitude constrained zones for agile spacecraft. Mathematic models for spacecraft using CMGs as actuators are developed firstly. Then, attitude constrained zones are formulated through unit-quaternion. Consequently, a convex potential function is proposed with a global minimum at the desired attitude and high potential close to the forbidden zones. To determine the gimbal rate that drives CMGs to generate commanded control torque from attitude controller and escape CMG singularity, general singular robust (GSR) steering law is employed. Finally, numerical simulation using the Kent Ridge 1 satellite as model is carried out to show the effectiveness of the proposed attitude control system.

II. Spacecraft Mathematic Model

In this paper, the unit-quaternion representation is used to describe the orientation of a spacecraft. A simple block dia-

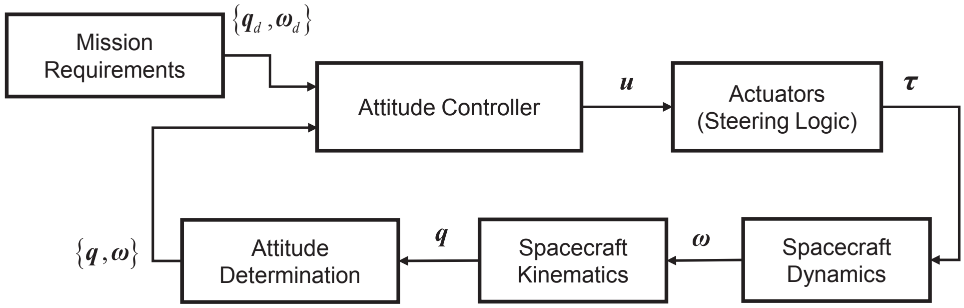

Fig. 1. A CMGs-based attitude control system.

gram representation of a CMGs-based attitude control system is illustrated in Figure 1.

A. Dynamics Equation with CMGs

When CMGs are used as actuator for attitude control, the total angular momentum is made up of the spacecraft main body angular momentum and the actuator angular momentum, which can be expressed in the body fixed frame as follows

$$\boldsymbol{H} = \boldsymbol{J}\boldsymbol{\omega} + \boldsymbol{A}\boldsymbol{h}, \tag{1}$$

where $\boldsymbol{J}$ is the inertia tensor, $\boldsymbol{\omega}$ is the inertial angular velocity vector of the spacecraft with respect to an inertial frame $\mathcal{I}$ and expressed in the body frame $\mathcal{B}$, $\boldsymbol{A}$ is the transformation matrix from the wheel frame to spacecraft body frame, $\boldsymbol{h}$ is the angular momentum produced by CMGs cluster. The equations of motion are derived by taking the time derivative of the total angular momentum of the system. The time derivative of $\boldsymbol{H}$ in the body frame is

$$\boldsymbol{J}\dot{\boldsymbol{\omega}} + \boldsymbol{\omega}^{\times}\boldsymbol{J}\boldsymbol{\omega} = \boldsymbol{\tau} + \boldsymbol{T}_{ext} \tag{2}$$

$$\boldsymbol{\tau} = -(\dot{\boldsymbol{A}}\boldsymbol{h} + \boldsymbol{A}\dot{\boldsymbol{h}}) - \boldsymbol{\omega}^{\times}\boldsymbol{A}\boldsymbol{h} \tag{3}$$

where $\boldsymbol{T}_{ext}$ is external torque such as external disturbances, $\boldsymbol{\tau}$ is the internal control torque generated by CMGs. The notation $\boldsymbol{a}^{\times}$ for a vector $\boldsymbol{a} = [a_1 \quad a_2 \quad a_3]^T$ is used to represent the skew-symmetric matrix

$$\boldsymbol{a}^{\times} = \begin{bmatrix} 0 & -a_3 & a_2 \\ a_3 & 0 & -a_1 \\ -a_2 & a_1 & 0 \end{bmatrix}. \tag{4}$$

A CMG contains a spinning rotor with large angular momentum, but whose angular momentum vector (direction) can be changed with respect to the spacecraft by gimballing the spinning rotor. A typical single gimbal control moment gyro (SGCMG) is shown in Figure 2, in which the rotor spins at a constant speed. The angular moment vector $\boldsymbol{h}_i$ points along the spindle axis, the gimbal axis is always orthogonal to the spin axis and is denoted by $\boldsymbol{g}_i$, the output torque axis $\boldsymbol{t}_i = \boldsymbol{g}_i \times \boldsymbol{h}_i$ is orthogonal to both $\boldsymbol{g}_i$ and $\boldsymbol{h}_i$. The subscript i denotes the ith SGCMG. Vectors $\boldsymbol{g}_i$, $\boldsymbol{h}_i$ and $\boldsymbol{t}_i$ form the right hand orthogonal CMG frame and they are the unit vector in their direction. The CMG is a torque amplification device as a small gimbal torque input produces a large control torque output on the spacecraft. Because CMGs are capable of generating large control torques and angular momentum, they are often favored for precision pointing and tracking control of agile spacecraft in low Earth orbit.

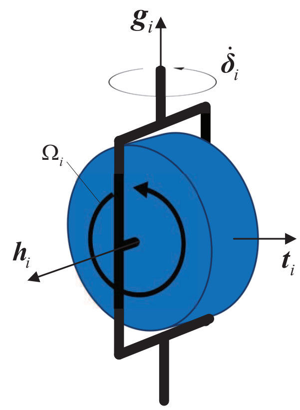

Fig. 2. Single gimbal control moment gyro.

For three-axis attitude control of spacecraft, four SGCMGs in a pyramid configuration are usually selected, and the skew angle is chosen as $\beta = 54.73$ deg so that the momentum envelope is nearly spherical. Assuming that the angular momentum vector of each SGCMG has the same magnitude h_0, the total angular momentum is expressed as

$$\begin{aligned} \boldsymbol{h}_{CMG} &= \boldsymbol{h}_1 + \boldsymbol{h}_2 + \boldsymbol{h}_3 + \boldsymbol{h}_4 \\ &= \boldsymbol{A}[\ h_0 \quad h_0 \quad h_0 \quad h_0\ ]^T, \end{aligned} \tag{5}$$

where $\boldsymbol{A}$ is the transformation matrix from the gimbal frame to spacecraft body frame given by

$$\boldsymbol{A} = \begin{bmatrix} -c\beta\sin\delta_1 & -\cos\delta_2 & c\beta\sin\delta_3 & \cos\delta_4 \\ \cos\delta_1 & -c\beta\sin\delta_2 & -\cos\delta_3 & c\beta\sin\delta_4 \\ s\beta\sin\delta_1 & s\beta\sin\delta_2 & s\beta\sin\delta_3 & s\beta\sin\delta_4 \end{bmatrix}$$

with $c\beta \equiv \cos\beta$, $s\beta \equiv \sin\beta$. The transformation matrix $\boldsymbol{A}$ of SGCMG is in general a function of CMG gimbal angle $\boldsymbol{\delta}$.

Specifically, for SGCMGs, since each flywheel has a constant spinning speed, it is clear that $\boldsymbol{A}\dot{\boldsymbol{h}} = 0$. Moreover, the time derivative of the transformation $\boldsymbol{A}$ is obtained as

$$\dot{\boldsymbol{A}} = \overline{\boldsymbol{A}}\dot{\boldsymbol{\delta}}, \tag{6}$$

where $\overline{\boldsymbol{A}}$ is the Jacobian matrix defined as

$$\overline{\boldsymbol{A}} = \begin{bmatrix} -c\beta\cos\delta_1 & \sin\delta_2 & c\beta\cos\delta_3 & -\sin\delta_4 \\ -\sin\delta_1 & -c\beta\cos\delta_2 & \sin\delta_3 & c\beta\cos\delta_4 \\ s\beta\cos\delta_1 & s\beta\cos\delta_2 & s\beta\cos\delta_3 & s\beta\cos\delta_4 \end{bmatrix}.$$

Therefore, the internal control torque $\boldsymbol{\tau}$ generated by SGCMGs in (3) is reduced to

$$\boldsymbol{\tau} = -h_0\overline{\boldsymbol{A}}\dot{\boldsymbol{\delta}} - \boldsymbol{\omega}^{\times}\boldsymbol{A}\boldsymbol{h}_{CMG}. \tag{7}$$

B. Kinematics Equation

The spacecraft kinematics in terms of unit-quaternion can be given by

$$\dot{\boldsymbol{Q}} = \frac{1}{2}\boldsymbol{Q}\otimes\boldsymbol{\nu}(\boldsymbol{\omega}) = \frac{1}{2}\begin{bmatrix}\boldsymbol{S}(\boldsymbol{q}) + q_0\boldsymbol{I}_3 \\ -\boldsymbol{q}^T\end{bmatrix}\boldsymbol{\omega}, \tag{8}$$

where $\boldsymbol{Q} = [q_1\ q_2\ q_3\ q_0]^T = [\boldsymbol{q}^T\ q_0]^T \in \mathbb{Q}_u$ denotes the unit-quaternion describing the attitude orientation of the body frame $\mathcal{B}$ with respect to inertial frame $\mathcal{I}$ and satisfies the constraint $\boldsymbol{q}^T\boldsymbol{q} + q_0^2 = 1$, $\boldsymbol{\nu}$: $\mathbb{R}^3 \to \mathbb{R}^4$ is defined as the mapping $\boldsymbol{\nu}(\boldsymbol{\omega}) = [\boldsymbol{\omega}^T\ 0]^T$.

Let $\boldsymbol{Q}_d \in \mathbb{Q}_u$ denote the desired attitude. In this paper, the rest-to-rest attitude reorientation problem of rotating a rigid spacecraft from its current attitude $\boldsymbol{Q}$ to a desired attitude $\boldsymbol{Q}_d$ is considered. The unit-quaternion error $\boldsymbol{Q}_e \in \mathbb{Q}_u$ is defined as $\boldsymbol{Q}_e = \boldsymbol{Q}_d^*\otimes\boldsymbol{Q} = [\boldsymbol{q}_e^T\ q_{e0}]^T$, which describes the discrepancy between the actual unit-quaternion $\boldsymbol{Q}$ and the desired unit-quaternion $\boldsymbol{Q}_d$. The kinematics represented by unit-quaternion error is described as [13]

$$\dot{\boldsymbol{Q}}_e = \frac{1}{2}\boldsymbol{Q}_e\otimes\boldsymbol{\nu}(\boldsymbol{\omega}_e), \tag{9}$$

where $\boldsymbol{\omega}_e = \boldsymbol{\omega} - \boldsymbol{R}(\boldsymbol{Q}_e)^T\boldsymbol{\omega}_d$, $\boldsymbol{R}(\boldsymbol{Q}_e)$ is the unit-quaternion error $\boldsymbol{Q}_e$ related rotation matrix [14] defined as $\boldsymbol{R}(\boldsymbol{Q}_e) = (q_{e0}^2 - \boldsymbol{q}_e^T\boldsymbol{q}_e)\boldsymbol{I}_3 + 2\boldsymbol{q}_e\boldsymbol{q}_e^T - 2q_{e0}\boldsymbol{S}(\boldsymbol{q}_e)$, and $\boldsymbol{\omega}_d$ denotes the desired angular velocity. In this paper, since rest-to-rest attitude reorientation problem is only considered, the desired angle velocity is $\boldsymbol{\omega}_d = 0$, which yields $\boldsymbol{\omega}_e = \boldsymbol{\omega}$. Therefore, the attitude error kinematics for rest-to-rest attitude reorientation maneuver in (9) can be rewritten as

$$\dot{\boldsymbol{Q}}_e = \frac{1}{2}\boldsymbol{Q}_e\otimes\boldsymbol{\nu}(\boldsymbol{\omega}) = \frac{1}{2}\begin{bmatrix}\boldsymbol{S}(\boldsymbol{q}_e) + q_{e0}\boldsymbol{I}_3 \\ -\boldsymbol{q}_e^T\end{bmatrix}\boldsymbol{\omega}. \tag{10}$$

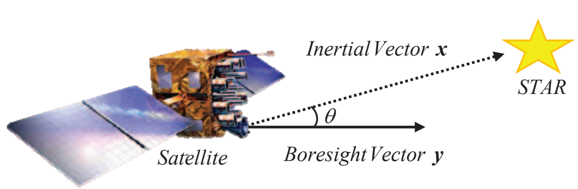

Fig. 3. Demonstration of attitude constraint.

C. Attitude Constraints

Suppose a half-cone angle strictly greater than θ should be maintained between the normalized boresight vector $\boldsymbol{y}$ of the spacecraft instrument and the normalized vector $\boldsymbol{x}$ pointing toward a certain celestial object, as shown in Fig. 3. This means that the cones with an apex angle of θ emanating from the sensitive on-board instruments should exclude the bright objects during the reorientation maneuver. When the attitude of the spacecraft is determined by $\boldsymbol{Q}$, the new boresight vector of the instrument in the inertial coordinates is

$$\boldsymbol{y}_I = (q_0^2 - \boldsymbol{q}^T\boldsymbol{q})\boldsymbol{y} + 2(\boldsymbol{q}^T\boldsymbol{y})\boldsymbol{q} + 2q_0(\boldsymbol{q}\times\boldsymbol{y}). \tag{11}$$

Then the constraints can be expressed by the vector dot product

$$\boldsymbol{x}\cdot\boldsymbol{y}_I < \cos(\theta), \tag{12}$$

Consequently, it follows from (12) that

$$q_0^2\boldsymbol{x}^T\boldsymbol{y} - \boldsymbol{q}^T\boldsymbol{q}\boldsymbol{x}^T\boldsymbol{y} + 2(\boldsymbol{q}^T\boldsymbol{y})\boldsymbol{x}^T\boldsymbol{q} + 2q_0\boldsymbol{q}^T(\boldsymbol{y}\times\boldsymbol{x}) < \cos(\theta) \tag{13}$$

which can be further rewritten as

$$\boldsymbol{Q}^T\begin{bmatrix}\boldsymbol{x}\boldsymbol{y}^T + \boldsymbol{y}\boldsymbol{x}^T - (\boldsymbol{x}^T\boldsymbol{y})\boldsymbol{I}_3 & \boldsymbol{y}\times\boldsymbol{x} \\ (\boldsymbol{y}\times\boldsymbol{x})^T & \boldsymbol{x}^T\boldsymbol{y}\end{bmatrix}\boldsymbol{Q} < \cos(\theta). \tag{14}$$

Suppose there are i constrained objectives associated with the jth on-board sensitive instrument in the spacecraft rotational space. Then, the spacecraft attitude $\boldsymbol{Q}\in\mathbb{Q}_u$ for which the boresight vector $\boldsymbol{y}_j$ with respect to the ith celestial object should satisfy the following constraint

$$\boldsymbol{Q}^T\boldsymbol{M}_i^j\boldsymbol{Q} < \cos(\theta_i^j), \tag{15}$$

where

$$\boldsymbol{M}_i^j = \begin{bmatrix} A_i^j & b_i^j \\ b_i^{jT} & d_i^j\end{bmatrix} \tag{16}$$

with

$$\begin{aligned} A_i^j &= \boldsymbol{x}_i\boldsymbol{y}_j^T + \boldsymbol{y}_j\boldsymbol{x}_i^T - (\boldsymbol{x}_i^T\boldsymbol{y}_j)\boldsymbol{I}_3, \\ b_i^j &= \boldsymbol{y}_j\times\boldsymbol{x}_i, \quad d_i^j = \boldsymbol{x}_i^T\boldsymbol{y}_j, \\ i &= 1,2,\ldots,n, \quad j = 1,2,\ldots,m. \end{aligned} \tag{17}$$

Subsequently, to represent the possible attitude for the jth instrument and the ith celestial object, a subset $\mathbb{Q}_{p_i^j}$ of $\mathbb{Q}_u$ is specified as

$$\mathbb{Q}_{p_i^j} = \{\boldsymbol{Q}\in\mathbb{Q}_u \mid \boldsymbol{Q}^T\boldsymbol{M}_i^j\boldsymbol{Q} - \cos\theta_i^j < 0\}. \tag{18}$$

The angle θ_i^j is the constraint angle about the direction of the ith object specified by $\boldsymbol{x}_i$ for the jth instrument boresight vector $\boldsymbol{y}_j$. Without loss of generality, the domain of the angle θ_i^j for all i and j is restricted to be $(0,\pi)$.

III. Attitude Controller and CMG Steering Logics Design

A. Potential Function Design

The potential function $V(\boldsymbol{Q})$: $\mathbb{Q}_p \to \mathbb{R}$, is defined as

$$V(\boldsymbol{Q}) = \|\boldsymbol{Q}_d - \boldsymbol{Q}\|^2 \sum_{j=1}^{m}\sum_{i=1}^{n} \frac{1}{\alpha(\boldsymbol{Q}^T\boldsymbol{M}_i^j\boldsymbol{Q} - \cos\theta_i^j)^2}, \quad (19)$$

where the set $\mathbb{Q}_p = \{\boldsymbol{Q} \in \mathbb{Q}_u \mid \boldsymbol{Q} \in \mathbb{Q}_{p_i^j}\}$ $(i = 1, 2, \ldots, n$, and $i = 1, 2, \ldots, m)$ represents the possible attitudes of the spacecraft on which the boresight vector of the onboard instruments lie outside of the constrained attitude.

Lemma 1: The potential function in (19) has the following properties:

1) $V(\boldsymbol{Q}_d) = 0$
2) $V(\boldsymbol{Q}) > 0$, for all $\boldsymbol{Q} \in \mathbb{Q}_p \backslash \{\boldsymbol{Q}_d\}$
3) $\nabla^2 V(\boldsymbol{Q}) > 0$ is positive definite for all $\boldsymbol{Q} \in \mathbb{Q}_p$ and $\boldsymbol{Q}_d \in \mathbb{Q}_p$.

The above three properties show that the potential function $V(\boldsymbol{Q})$ defined in (19) is smooth and strictly convex for all $\boldsymbol{Q} \in \mathbb{Q}_p$ and $\boldsymbol{Q}_d \in \mathbb{Q}_p$, and it has a global minimum at $\boldsymbol{Q} = \boldsymbol{Q}_d$.

B. Attitude Controller Design

The attitude regulation controller is designed as

$$\boldsymbol{\tau} = -k_1\boldsymbol{\omega} - k_2\boldsymbol{q}_e + k_3 \mathrm{Vec}[\nabla V^* \otimes \boldsymbol{Q}] \quad (20)$$

where the operator Vec[·] denotes the vector part of [·].

Consider the following Lyapunov candidate:

$$V_\ell = \frac{1}{2}\boldsymbol{\omega}^T\boldsymbol{J}\boldsymbol{\omega} + k_2[\boldsymbol{q}_e^T\boldsymbol{q}_e + (1 - \boldsymbol{q}_{e0})^2] + 2k_3 V(\boldsymbol{Q}). \quad (21)$$

The time derivative of V_ℓ is

$$\begin{aligned}\dot{V}_\ell &= \boldsymbol{\omega}^T\boldsymbol{J}\dot{\boldsymbol{\omega}} + 2k_3\nabla V^T(\frac{1}{2}\boldsymbol{Q} \otimes \boldsymbol{\nu}(\boldsymbol{\omega})) \\ &= \boldsymbol{\omega}^T\big\{-\boldsymbol{S}(\boldsymbol{\omega})\boldsymbol{J}\boldsymbol{\omega} + k_2\boldsymbol{q}_e + \boldsymbol{\tau}\big\} + k_3\boldsymbol{\nu}(\boldsymbol{\omega})^T(\boldsymbol{Q}^* \otimes \nabla V).\end{aligned}$$

From $\boldsymbol{\omega}^T\boldsymbol{S}(\boldsymbol{\omega})(\boldsymbol{J}_0\boldsymbol{\omega} + \boldsymbol{\delta}^T\psi) = 0$, it is obtained that

$$\dot{V}_\ell = \boldsymbol{\omega}^T(k_2\boldsymbol{q}_e + \boldsymbol{\tau}) + k_3\boldsymbol{\nu}(\boldsymbol{\omega})^T(\boldsymbol{Q}^* \otimes \nabla V). \quad (22)$$

Note that

$$\boldsymbol{\nu}(\boldsymbol{\omega})^T(\boldsymbol{Q}^* \otimes \nabla V) = -\boldsymbol{\omega}^T\mathrm{Vec}[(\nabla V^* \otimes \boldsymbol{Q})], \quad (23)$$

and substituting the control law (20) into (22) yields

$$\dot{V}_\ell = -k_1\boldsymbol{\omega}^T\boldsymbol{J}\boldsymbol{\omega}. \quad (24)$$

Therefore, it is clear from (24) that $\boldsymbol{Q}_e$, $\boldsymbol{\omega}$, and $V(\boldsymbol{Q})$ are bounded. Consequently, one can obtain that $\ddot{V}_\ell$ is bounded. Hence, according to Barbalat's Lemma, one can conclude that $\lim_{t\to\infty} \boldsymbol{\omega} = 0$. In addition, since the potential $V(\boldsymbol{Q})$ is strictly convex, the following equivalence is ensured

$$\{\boldsymbol{Q} \mid \nabla V(\boldsymbol{Q}) = \nabla V^*(\boldsymbol{Q}) = 0\} \Leftrightarrow \{\boldsymbol{Q} \mid V(\boldsymbol{Q}) = 0\}, \quad (25)$$

which consequently implies that $\lim_{t\to\infty} \boldsymbol{Q}(t) = \boldsymbol{Q}_d$.

In summary, we have the following theorem.

Theorem 1: Consider the spacecraft attitude control systems expressed by (2) and (8) in the presence of attitude constrained zones. The commanded control torque generated by controller (20) guarantees that all closed-loop signals are bounded and that $\lim_{t\to\infty} \boldsymbol{\omega} = 0$ and $\lim_{t\to\infty} \boldsymbol{Q}(t) = \boldsymbol{Q}_d$.

C. Steering Logic for CMGs

The steering logic transfers the control torques from system level to actuator level. Assuming that the commanded control torque $\boldsymbol{u}$ is computed by a proper attitude controller for achieving the desired three-axis attitude maneuver, then the steering law should be designed such CMGs realize the commanded control torque, i.e., $\boldsymbol{\tau} = \boldsymbol{u}$. One of the major issues in using CMGs for spacecraft attitude control is the CMG geometric singularity problem in which no control torque is generated for the commanded control torque along a particular direction.

Based on the equation in (7), the following relation can be obtained

$$\boldsymbol{\tau} = \boldsymbol{u} = -h_0\overline{\boldsymbol{A}}\dot{\boldsymbol{\delta}} - \boldsymbol{\omega}^\times\boldsymbol{A}\boldsymbol{h}_{CMG}. \quad (26)$$

It means that the CMG steering logic should determine the gimbal rate $\dot{\boldsymbol{\delta}}$ that can generate the commanded control torque $\boldsymbol{u}$. The basic solution of $\dot{\boldsymbol{\delta}}$ for above equation is referred to as the peseudoinverse steering logic, which is given by

$$\dot{\boldsymbol{\delta}} = -\frac{1}{h_0}\overline{\boldsymbol{A}}^\dagger(\boldsymbol{u} + \boldsymbol{\omega}^\times\boldsymbol{A}\boldsymbol{h}_{CMG}), \quad (27)$$

where the peseudoinverse is defined as $\overline{\boldsymbol{A}}^\dagger = \overline{\boldsymbol{A}}^T(\overline{\boldsymbol{A}}\,\overline{\boldsymbol{A}}^T)^{-1}$. As mentioned earlier that the Jacobian matrix $\overline{\boldsymbol{A}}$ is a function of gimbal angle $\boldsymbol{\delta}$, the CMG steering logic may encounter singularity if rank$(\overline{\boldsymbol{A}}) < 3$ for certain sets of gimbal angles.

Several approaches for avoiding or escaping CMGs singular states have been proposed in literature. Here, one of the most commonly used method, the general singular robust (GSR) steering law [2], is employed to handle CMG singularity. According to GSR steering law, the gimbal rate that can generate the commanded torque is given by

$$\dot{\boldsymbol{\delta}} = -\frac{1}{h_0}\overline{\boldsymbol{A}}^\sharp\left(\boldsymbol{u} + \boldsymbol{\omega}^\times\boldsymbol{A}\boldsymbol{h}_{CMG}\right), \quad (28)$$

where $\overline{\boldsymbol{A}}^\sharp = \overline{\boldsymbol{A}}^T\left[\overline{\boldsymbol{A}}\,\overline{\boldsymbol{A}}^T + \alpha\boldsymbol{E}\right]^{-1}$, $\alpha = \alpha_0\exp\left(-\mu m^2\right)$, $m = \sqrt{\det\left(\overline{\boldsymbol{A}}\,\overline{\boldsymbol{A}}^T\right)}$ is the singularity measure. The matrix $\boldsymbol{E}$ is defined as

$$\boldsymbol{E} = \begin{bmatrix} 1 & \varepsilon_3 & \varepsilon_2 \\ \varepsilon_3 & 1 & \varepsilon_1 \\ \varepsilon_2 & \varepsilon_1 & 1 \end{bmatrix}, \quad \varepsilon_i = \varepsilon_0\sin(\varpi_i t + \phi_i) \quad (29)$$

where ε_i, ϖ_i and ϕ_i are properly selected.

IV. Numerical Simulation

A. Simulation Specification

In this section, satellite attitude control with CMGs is studied through simulation. The Kent Ridge 1 (KR-1) satellite is considered as simulation model. Table I contains the satellite parameters used for the simulations.

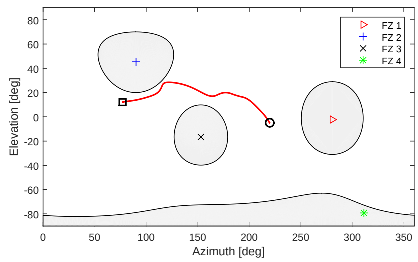

Fig. 4. Trajectory of sensitive instrument pointing direction in 2D cylindrical projection.

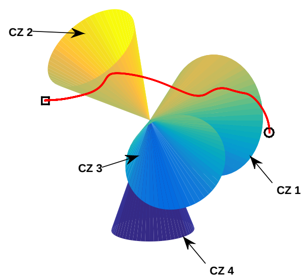

Fig. 5. Trajectory of sensitive instrument pointing direction in 3D.

TABLE I
SIMULATION PARAMETERS

Parameter	value
Mass (kg)	79
Size (mm)	575×572×384
Moment of inertia (kg·m^2)	$J_1 = 3.34,\ J_2 = 5.29,\ J_3 = 3.21$

TABLE II
SGCMGS PARAMETERS

Parameter	value
Skew angle (deg)	54.74
Maximum momentum (Nms)	$h_{\max} = 2$
Maximum gimbal rate (deg/s)	$\dot{\delta}_{\max} = 30$

Four SGCMGs in a regular pyramid configuration is used in simulation. The specification of SGCMG is shown in Table II. The initial gimbal angles are selected as $\boldsymbol{\delta}(0) = [0 \quad 0 \quad 0 \quad 0]^T$ deg, which are far way from singular states. The parameters in GSR steering law described in equation (28) are selected as:

$$\alpha_0 = 0.01, \quad \mu = 10, \quad \phi_1 = 0, \quad \phi_2 = \frac{\pi}{2}, \quad \phi_3 = \pi,$$
$$\epsilon_i = 0.01 \sin(0.5\pi t + \phi_i), \quad i = 1, 2, 3. \tag{30}$$

The spacecraft is retargeting its sensitive instrument (such as infrared telescopes or interferometers) while avoiding four

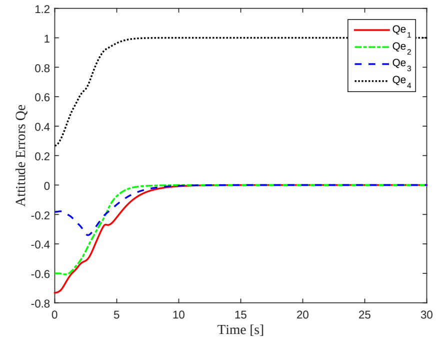

Fig. 6. Quaternion error.

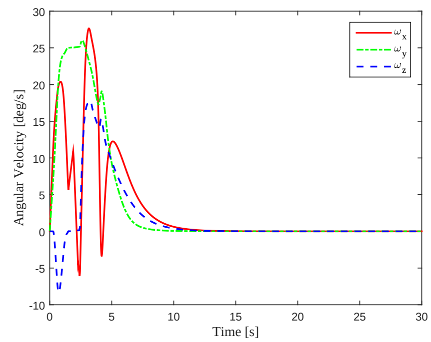

Fig. 7. Angular velocity.

celestial objects (such as sun light or other bright objects) in the spacecraft reorientation configuration space. Four attitude-constrained zones are chosen without overlapping with each other. The details of the four attitude-constrained zones are given in Table III, in which the normalized vectors pointing toward the corresponding celestial objects are expressed with respect to the inertial frame. Both initial and desired attitude are chosen such that they are out of four attitude-constrained zones. The spacecraft is assumed to have the initial attitude $\boldsymbol{Q}(0) = [0.329\ 0.659\ \ -0.619\ \ -0.2726]^T$ and initial angular velocity $\boldsymbol{\omega}(0) = [0\ 0\ 0]^T$ rad/s. The controller gains in (20) are chosen as $k_1 = 3.64\boldsymbol{J}$, $k_2 = 4\boldsymbol{J}$, and $k_3 = 0.005\boldsymbol{J}$.

TABLE III
SIMULATION PARAMETERS

Constrained Zone (CZ)	Constrained Object	Angle
CZ 1	[0.183 -0.983 -0.036]	30 deg
CZ 2	[0 0.707 0.707]	25 deg
CZ 3	[-0.853 0.436 -0.286]	25 deg
CZ 4	[0.122 -0.140 -0.983]	20 deg

B. Simulation Results

The simulation results are shown in Figures 4 to 10. The desired attitude of the flexible spacecraft rotating to is selected as $\boldsymbol{Q}_d = [0.5\ \ -0.55\ \ -0.42\ \ -0.5207]^T$. Fig. 4 depicts the same trajectories on the cylindrical projection of the corresponding

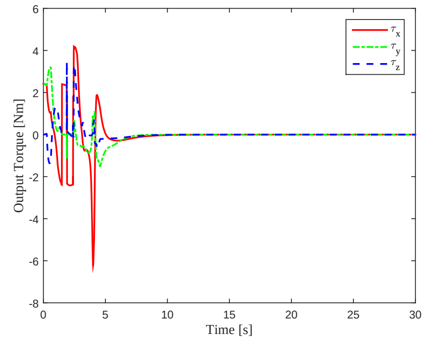

Fig. 8. Commanded control torque from attitude controller.

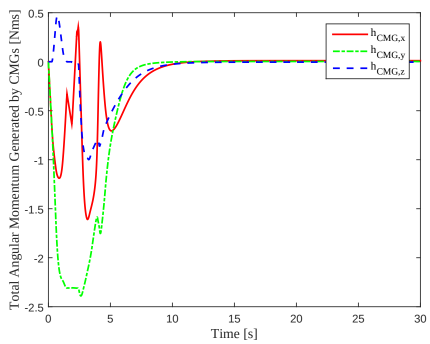

Fig. 9. Angular momentum generated by CMGs.

celestial spheres. Fig. 5 shows the trajectory of sensitive instrument pointing direction in 3D during the rest-to-rest attitude maneuver, in which four attitude-constrained zones in Table III are plotted inside a celestial sphere. As shown Figs. 4 and 5, the reorientation trajectory generated by the proposed controller in (20) avoids all four constrained zones while achieving the desired attitude. Figs. 6 to 8 describes details of the control performance in Case I, where the time histories for attitude error, angular velocity, and commanded control torque are illustrated. It can be observed that the proposed attitude controller in (20) obtains a satisfactory performance in the spacecraft rest-to-rest reorientation despite four attitude-constrained zones. Angular momentum provided by CMGs are shown in Figure 9. Figure 10 shows the gimbal angle response during the attitude maneuver.

V. Conclusions

In this paper, a potential function based attitude controller is developed for agile spacecraft to achieve rest-to-rest attitude slew while avoiding the attitude constrained zones . In order to have a fast attitude maneuver, CMG that has a property of large torque amplification is utilized as actuators in attitude control systems. In view of CMG working principle, mathematic models for spacecraft using CMGs are established. A potential function parameterized by unit-quaternion is then proposed with a global minimum at the desired attitude and high potential close to attitude forbidden zones. Nonlinear

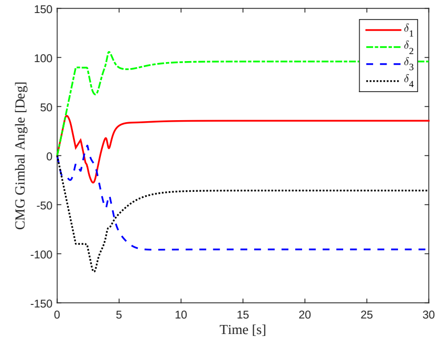

Fig. 10. Gimbal angle.

feedback control law and GSR steering law are formulated to guarantee three-axis attitude control and determine the gimbal rate, respectively. Through numerical simulation on the Kent Ridge 1 satellite, it has shown that fast and high precision attitude pointing maneuver can be achieved using the proposed attitude control systems.

References

[1] Q. Shen, D. W. Wang, S. Q. Zhu, and E. K. Poh, “Finite-time fault-tolerant attitude stabilization for spacecraft with actuator saturation,” *IEEE Transactions on Aerospace and Electronic Systems*, vol. 51, no. 3, pp. 2390 – 2405, 2015.

[2] B. Wie, D. Bailey, and C. Heiberg, “Singularity robust steering logic for redundant single-gimbal control moment gyros,” *Journal of Guidance, Control, and Dynamics*, vol. 24, no. 5, pp. 865–872, 2001.

[3] B. Wie, “Singularity analysis and visualization for single-gimbal control moment gyro systems,” *Journal of Guidance, Control, and Dynamics*, vol. 27, no. 2, pp. 271–282, 2004.

[4] K. A. Ford and C. D. Hall, “Singular direction avoidance steering for control-moment gyros,” *Journal of Guidance, Control, and Dynamics*, vol. 23, no. 4, pp. 648–656, 2000.

[5] B. Wie, “Singularity escape/avoidance steering logic for control moment gyro systems,” *Journal of Guidance, Control, and Dynamics*, vol. 28, no. 5, pp. 948–956, 2005.

[6] F. A. Leve and N. G. Fitz-Coy, “Hybrid steering logic for single-gimbal control moment gyroscopes,” *Journal of Guidance Control and Dynamics*, vol. 33, no. 4, pp. 1202–1212, 2010.

[7] B. Wie, “Singularity analysis and visualization for single-gimbal control moment gyro systems,” *Journal of Guidance, Control, and Dynamics*, vol. 27, no. 2, pp. 271–282, 2004.

[8] H. B. Hablani, “Attitude commands avoiding bright objects and maintaining communication with ground station,” *Journal of Guidance, Control, and Dynamics*, vol. 22, no. 6, pp. 759–767, Nov.-Dec. 1999.

[9] C. R. McInnes, “Large angle slew maneuvers with autonomous sun vector avoidance,” *Journal of Guidance, Control, and Dynamics*, vol. 17, no. 4, pp. 875–877, 1994.

[10] G. Avanzini, G. Radice, and I. Ali, “Potential approach for constrained autonomous manoeuvres of a spacecraft equipped with a cluster of control moment gyroscopes,” *Proceedings of the Institution of Mechanical Engineers, Part G: Journal of Aerospace Engineering*, vol. 223, no. 3, pp. 285–296, 2009.

[11] U. Lee and M. Mesbahi, “Feedbak control for spacecraft reorientation under attiude contstraints via convex potentials,” *IEEE Transactions on Aerospace and Electronic Systems*, vol. 50, no. 4, pp. 2578–2592, Oct. 2014.

[12] C. R. McInnes, “Nonlinear control for large angle attitude slew maneuver,” in *Proceedings of the Third ESA Symposium on Spacecraft Guidance, Navigationm and Control*, 1996, pp. 543–548.

[13] B. Wie, *Space Vehicle Dynamics and Control*. AIAA, Reston, VA: AIAA Education Series, 2008.

[14] M. J. Sidi, *Spacecraft Dynamics and Control*. Cambridge, U.K.: Cambridge, NY: Cambridge University Press, 1997.